

Structural Variants in the Low-Temperature β Phase of Stoichiometric Cuprous Selenide

JADRANKO GLADIĆ,¹ OGNJEN MILAT, ZLATKO VUČIĆ,
AND VLASTA HORVATIĆ

*Institute of Physics of the University of Zagreb, Bijenička cesta 46,
P. O. B. 304, 41000 Zagreb, Yugoslavia*

Received May 19, 1989; in revised form October 10, 1990

Symmetry lowering from $T_d^2(F\bar{4}3m)$ to $C_s^3(Cm)$ at $\alpha \rightarrow \beta$ first-order phase transition of the superionic conductor Cu_2Se is described by two nonequivalent wave vectors:

$$\mathbf{k}^R = \frac{2\pi}{a_c} \left(\frac{1}{2} \frac{1}{2} \frac{1}{2} \right) \quad \text{and} \quad \mathbf{k}^m = \frac{2\pi}{a_c} \left(\frac{1}{3} \frac{1}{3} 0 \right).$$

Four orientation variants of the rhombohedrally deformed cage sublattice are equally probable equilibrium structures which correspond to four rays in the star of \mathbf{k}^R . Such twinning was observed using a microfurnace built for the Weissenberg goniometer. Three monoclinic β -phase structure variants displaying together pseudorhombohedral symmetry can couple to each body cube diagonal as a cage distortion direction, giving a total of 12—the number of rays in the star of \mathbf{k}^m . © 1991 Academic Press, Inc.

Introduction

According to the generally accepted model (1–3) the high-temperature superionic α phase of the stoichiometric cuprous selenide Cu_2Se consists of an immobile subsystem—the cubic cage of $T_d^2(F\bar{4}3m)$ symmetry, built of four Se atoms in (a) and four Cu atoms in (c) positions—and a disordered mobile cation subsystem of the remaining Cu atoms statistically distributed over the cage interstitial sites.

The first-order phase transition to nonsuperionic β - Cu_2Se ($T_c = 413$ K) is marked by ordering of the mobile subsystem accom-

panied by the simultaneous deformation of the cage sublattice and 1.4% volume expansion (3, 4).

The results of structural investigations of the room temperature β phase of the stoichiometric cuprous selenide Cu_2Se have been reported in quite a number of papers offering several seemingly mutually inconsistent structural models [see Refs. in (3)]. In their paper, Milat *et al.* (3) elucidated the origin of these discrepancies, and described the ordered β -phase structure as monoclinic [space group $C_s^3(Cm)$], inferring from the symmetry displayed in the single crystal Weissenberg photographs and electron diffraction (ED) patterns at room temperature.

Three monoclinic superlattice orientation variants differing by $\pm 120^\circ$ rotations around a threefold symmetry axis of the cubic cage

¹ To whom correspondence should be addressed.

sublattice were simultaneously present in the ED patterns, displaying the enhanced overall symmetry. Along this distinguished axis ($[111]_c$) a slight elongation of the cage sublattice occurred, reducing the cage sublattice symmetry from cubic T_d^2 ($F\bar{4}3m$) to rhombohedral C_{3v}^5 ($R3m$) (3–5). Upon completing the $\beta \rightarrow \alpha \rightarrow \beta$ heating and cooling cycle repeatedly, three analogous monoclinic orientation variants were always observed, but sometimes coupled to any other of the four body cube diagonals as the cage distortion direction.

Facing such richness of observed ordering possibilities, we feel the need to clarify the questions arising about the possible number of the structure orientation variants that are formed upon the $\alpha \rightarrow \beta$ phase transition and their mutual relationships and transformations.

Group-Theoretical Considerations

We consider the symmetry changes in the transition between two phases of stoichiometric cuprous selenide using the general group-theoretical approach within the framework of the Landau theory of phase transitions (6–8).

The space group G of the disordered parent phase (high-temperature α -Cu₇Se) is T_d^2 ($F\bar{4}3m$). The symmetric set of primitive translation vectors for this FCC lattice is given as $\mathbf{a}_1 = a_c(\frac{1}{2}\hat{y} + \frac{1}{2}\hat{z}) = a_c(0\frac{1}{2}\frac{1}{2})$, $\mathbf{a}_2 = a_c(\frac{1}{2}0\frac{1}{2})$, $\mathbf{a}_3 = a_c(\frac{1}{2}\frac{1}{2}0)$ (a_c being the length of the conventional cubic cell edge), and the primitive cell volume is $V_c = \frac{1}{4}a_c^3$. The corresponding reciprocal lattice vectors are $\mathbf{a}_1^* = (2\pi/a_c)(\bar{1}11)$, $\mathbf{a}_2^* = (2\pi/a_c)(1\bar{1}1)$, $\mathbf{a}_3^* = (2\pi/a_c)(11\bar{1})$. The space group is symmorphic, containing only pure rotational operations which form the point group $G_O \equiv T_d$ ($\bar{4}3m$), with 24 elements in five classes (9) shown in Fig. 1.

For the moment we focus our attention only on the cage sublattice and consider sep-

arately the reduction of the cage sublattice symmetry from cubic to rhombohedral upon the $\alpha \rightarrow \beta$ phase transition. The matrix S_{cR} relating the rhombohedral cell vectors ($\mathbf{a}_R, \mathbf{b}_R, \mathbf{c}_R$) (row matrix 3×1) to the conventional cubic ones ($a_c\hat{x}, a_c\hat{y}, a_c\hat{z}$) is deduced from the single crystal X-ray diffraction patterns (5):

$$S_{cR} = \begin{bmatrix} 1 & \frac{1}{2} & \frac{1}{2} \\ \frac{1}{2} & 1 & \frac{1}{2} \\ \frac{1}{2} & \frac{1}{2} & 1 \end{bmatrix},$$

$$\det S_{cR} = \frac{1}{2}, V_R = \frac{1}{2}a_c^3 = 2V_c$$

$$(\mathbf{a}_R, \mathbf{b}_R, \mathbf{c}_R) = (a_c\hat{x}, a_c\hat{y}, a_c\hat{z}) \cdot S_{cR}$$

The reciprocal lattice vectors are $\mathbf{a}_R^* = (2\pi/a_c)(\frac{3}{2}\frac{1}{2}\frac{1}{2})$, $\mathbf{b}_R^* = (2\pi/a_c)(\frac{1}{2}\frac{3}{2}\frac{1}{2})$, $\mathbf{c}_R^* = (2\pi/a_c)(\frac{1}{2}\frac{1}{2}\frac{3}{2})$.

The basic vectors of the rhombohedral lattice are readily expressed as linear combinations of cubic primitive vectors, $\mathbf{a}_R = \mathbf{a}_2 + \mathbf{a}_3$, $\mathbf{b}_R = \mathbf{a}_3 + \mathbf{a}_1$, $\mathbf{c}_R = \mathbf{a}_1 + \mathbf{a}_2$, the translations of the rhombohedral lattice thus forming the subgroup of cubic translations.

The S_{cR} matrix relates a symmetry operator \mathbf{g} of the point group G_O [expressed in the reference frame ($a_c\hat{x}, a_c\hat{y}, a_c\hat{z}$)] to the same symmetry operator \mathbf{h} [expressed in the reference frame ($\mathbf{a}_R, \mathbf{b}_R, \mathbf{c}_R$)] if the operation is conserved after symmetry reduction (10):

$$\mathbf{h} = S_{cR}^{-1} \mathbf{g} S_{cR}.$$

Using the matrices of the Γ_5 three-dimensional representation (11) [that is, transformation of coordinates of the (x, y, z) point under the rotational symmetry operations from (7, 12)] for \mathbf{g} , we compute the matrices of \mathbf{h} . Those \mathbf{h} matrices that contain only ± 1 or 0 as their h_{ij} elements represent the symmetry operations conserved within the reduced symmetry structure. Application of the described procedure shows that the point group of the rhombohedrally distorted cubic cage sublattice is $H_O \equiv C_{3v}$ ($3m$).

The space group H of the described rhombohedral lattice is the symmorphic space

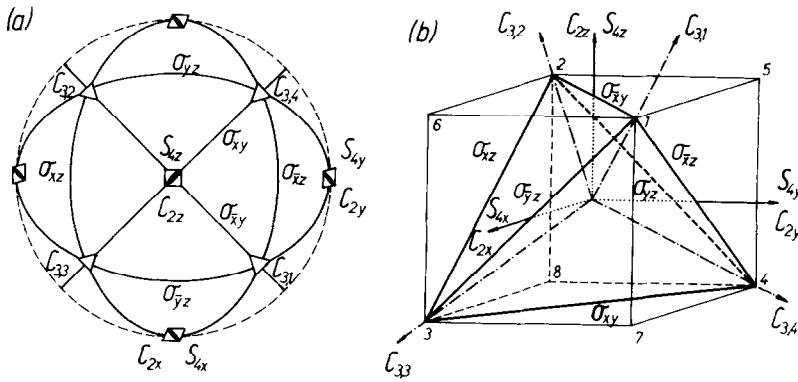


FIG. 1. (a) Stereographic projection of the point group $G_0 \equiv T_d (43m)$. (b) Symmetry elements of the point group $T_d (43m)$ shown in their exact positions with respect to the regular tetrahedron inscribed in a cube.

group $C_{3v}^5 (R3m)$, and is, as shown, the subgroup of the high symmetry structure space group $T_d^2 (F\bar{4}3m)$. This fulfills the I condition of Landau for a second-order phase transition (6–8).

The irreducible representation which describes the transition is found by inspecting the changes in translational symmetry. In this transition the primitive cell volume is doubled ($V_R = 2V_c$) and the doubling of periodicity is observed in the $[111]_c$ direction ($\mathbf{a}_R + \mathbf{b}_R + \mathbf{c}_R = a_c(222) = 2(\mathbf{a}_1 + \mathbf{a}_2 + \mathbf{a}_3)$). Thus, the transition corresponds to a representation with wave vector $\mathbf{k}^R = (2\pi/a_c) (\frac{1}{2}\frac{1}{2}\frac{1}{2}) = \frac{1}{2}(\mathbf{a}_1^* + \mathbf{a}_2^* + \mathbf{a}_3^*) = \mathbf{a}_R^* + \mathbf{b}_R^* + \mathbf{c}_R^*$. As $-\mathbf{k}^R = \mathbf{k}^R + (2\pi/a_c) (\bar{1}\bar{1}\bar{1})$, and $(2\pi/a_c) (\bar{1}\bar{1}\bar{1})$ is a cubic reciprocal lattice vector, the IV condition of Landau (7, 8) for a second-order phase transition is also satisfied. The function $\exp(i\mathbf{k}^R \cdot \mathbf{r}) = \exp(i\pi(x + y + z))$ (for $\mathbf{r} = x\hat{x} + y\hat{y} + z\hat{z}$) is a basis function for the translational symmetry operations that is symmetric with respect to the translations of rhombohedral structure and antisymmetric with respect to lost cubic translations. Such a change of structure described by a single reciprocal vector \mathbf{k}^R corresponds to a single irreducible representa-

tion of the space group G , thus satisfying the II condition of Landau.

The proper symmetry group of the wave vector is $C_{3v} \equiv H_0$, consisting of those rotational symmetry operations of G that leave \mathbf{k}^R invariant ($\{[E], [C_{3,1}^+, C_{3,1}^-], [\sigma_{xy}, \sigma_{xz}, \sigma_{yz}]\}$). The \mathbf{k}^R vector corresponds to the L symmetry point of the Brillouin zone of the FCC lattice and belongs to the star $\{\mathbf{k}^R 9\}$ consisting of four rays $\mathbf{k}_1^R = (2\pi/a_c) (\frac{1}{2}\frac{1}{2}\frac{1}{2})$, $\mathbf{k}_2^R = (2\pi/a_c) (\frac{1}{2}\frac{1}{2}\bar{1})$, $\mathbf{k}_3^R = (2\pi/a_c) (\frac{1}{2}\bar{1}\frac{1}{2})$, $\mathbf{k}_4^R = (2\pi/a_c) (\bar{1}\frac{1}{2}\frac{1}{2})$.

The possible changes of translational symmetry in phase transitions associated with all Brillouin zone special symmetry points of all types of Bravais lattices are tabulated in (13). The type of the Bravais lattice obtained upon lowering the symmetry is determined by the star of the wave vector characterizing the transition and the number of rays involved. For the lowering of the FCC structure symmetry corresponding to any one out of four rays of the $\{\mathbf{k}^R 9\}$ star, a rhombohedral cell of doubled volume is obtained [Tables 3.1 and 3.2 in (13)] with primitive translation vectors equal to those we deduced from Weissenberg photographs (5) (e.g., another transition including super-

TABLE I
FOR $\mathbf{g} \in G_0$, $H_j = \mathbf{g}^{-1} H_i \mathbf{g}$ (E.G., FOR $i = 1; j = 1-4$)

\mathbf{g}^{-1}	\mathbf{g}	\mathbf{g}^{-1}	\mathbf{g}	\mathbf{g}^{-1}	\mathbf{g}	\mathbf{g}^{-1}	\mathbf{g}
E	E	$C_{3,3}^{-1}$	$C_{3,3}^1$	$C_{3,4}^{-1}$	$C_{3,4}^1$	$C_{3,2}^{-1}$	$C_{3,2}^1$
$C_{3,1}^{-1}$	$C_{3,1}^1$	$C_{3,4}^1$	$C_{3,4}^{-1}$	$C_{3,2}^1$	$C_{3,2}^{-1}$	$C_{3,3}^1$	$C_{3,3}^{-1}$
$C_{3,1}^1$	$C_{3,1}^{-1}$	C_{2z}	C_{2z}	C_{2x}	C_{2x}	C_{2y}	C_{2y}
$\sigma_{\bar{x}y}$	$\sigma_{\bar{x}y}$	σ_{xy}	σ_{xy}	σ_{yz}	σ_{yz}	σ_{xz}	σ_{xz}
$\sigma_{\bar{x}z}$	$\sigma_{\bar{x}z}$	S_{4x}^{-1}	S_{4x}^1	S_{4y}^{-1}	S_{4y}^1	S_{4z}	S_{4z}^1
$\sigma_{\bar{y}z}$	$\sigma_{\bar{y}z}$	S_{4y}^1	S_{4y}^{-1}	S_{4z}^1	S_{4z}^{-1}	S_{4x}	S_{4x}^{-1}
$\mathbf{g}^{-1} H_1 \mathbf{g} = H_1$		$\mathbf{g}^{-1} H_1 \mathbf{g} = H_2$		$\mathbf{g}^{-1} H_1 \mathbf{g} = H_3$		$\mathbf{g}^{-1} H_1 \mathbf{g} = H_4$	
$\mathbf{g}^{-1} \in E H_1$		$\mathbf{g}^{-1} \in C_{2z} H_1$		$\mathbf{g}^{-1} \in C_{2x} H_1$		$\mathbf{g}^{-1} \in C_{2y} H_1$	
		$\in S_{4x}^{-1} H_1$		$\in S_{4y}^{-1} H_1$		$\in S_{4x}^1 H_1$	
		$\in S_{4y}^1 H_1$		$\in S_{4z}^1 H_1$		$\in S_{4z}^{-1} H_1$	

position of four rhombohedral orderings, that is according to all rays of the star, would result in a large FCC cell, with doubled cell edges and a cell volume eight times larger than that of the initial structure).

The other wave vectors in the star are obtained from \mathbf{k}_1^R by applying to it symmetry operators of the group G_0 not conserved in the H_0 subgroup (e.g., $E \mathbf{k}_1^R = \mathbf{k}_1^R$, $C_{2x} \mathbf{k}_1^R = \mathbf{k}_2^R$, $C_{2y} \mathbf{k}_1^R = \mathbf{k}_3^R$, $C_{2z} \mathbf{k}_1^R = \mathbf{k}_4^R$). These operators form a so-called variant generating group (V.G.G.) (14), which is a group formed by coset representatives in the decomposition of G_0 into cosets of H_0 . The choice of coset representatives is not unique in this case, so that the following decompositions are possible:

$$\begin{aligned}
 G_0 &= E H_0 + C_{2x} H_0 + C_{2y} H_0 \\
 &\quad + C_{2z} H_0 = D_2 \wedge C_{3v} \\
 &= E H_0 + C_{2x} H_0 + S_{4x}^1 H_0 \\
 &\quad + S_{4x}^{-1} H_0 = S_4^{(x)} \cdot C_{3v} \\
 &= E H_0 + S_{4y}^{-1} H_0 + C_{2y} H_0 \\
 &\quad + S_{4y}^1 H_0 = S_4^{(y)} \cdot C_{3v} \\
 &= E H_0 + S_{4z}^1 H_0 + S_{4z}^{-1} H_0 \\
 &\quad + C_{2z} H_0 = S_4^{(z)} \cdot C_{3v}.
 \end{aligned}$$

The number of coset representatives in a decomposition is equal to the index of group H_0 in G_0 . Application of one of the coset representatives \mathbf{g}_i to the structure of the lower symmetry phase gives a structure of the space group symmetry $\mathbf{g}_i H \mathbf{g}_i^{-1}$ (Table I). The space groups of the four structures thus obtained are distinct but equivalent (15, 16) subgroups of G in the sense that their elements differ in orientation (Fig. 2). All H_i ($i = 1, 2, 3, 4$) groups are crystallographically equivalent and related by symmetry operations of G_0 —they are the four possible orientation (twin) variants (14, 16) or coherent domains (16) of the ordered structure. (It can be easily checked in Table I that D_2 , $S_4^{(x)}$, $S_4^{(y)}$, and $S_4^{(z)}$ generate the same set of variants, although by using different symmetry operations of G_0 .) The appearance of a specific orientation variant corresponds to the transition with the appropriate single ray of the $\{\mathbf{k}^R\}$ star involved.

These four variants represent the four available choices of one cubic threefold axis as the direction of the uniaxial distortion (3, 4) of the cubic cage sublattice (compare Fig. 2 with Fig. 1.).

The basis functions for the irreducible representation (irr. rep.) of the entire space group G associated with the vector \mathbf{k}^R are

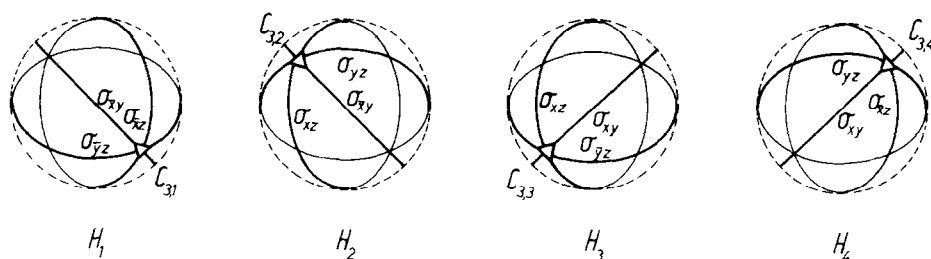


FIG. 2. Stereographic projection of the subgroup $H_0 \equiv C_{3v} (3m)$ showing exactly the four possible orientations with respect to the G_0 group $T_d (43m)$ (compare with Fig. 1a).

obtained by subjecting the mentioned basis function for the translational symmetry operations to all rotational symmetry operations of the group. The elements of the point group of the wave vector transform it according to the totally symmetric small rep. of the group of the wave vector $\mathbf{k}_1^R = (2\pi/a_c) (\frac{1}{2}\frac{1}{2}\frac{1}{2})$ [one-dimensional loaded rep. $\hat{\tau}^1$ of the wave vector \mathbf{k}_0 of the T_d^2 space group (12)]. The remaining elements of the point group T_d transform this basis function into one of the basis functions associated with the wave vectors of the same star [$\exp(i\pi(x+y+z))$, $\exp(i\pi(x-y-z))$, $\exp(i\pi(-x+y-z))$, $\exp(i\pi(-x-y+z))$] corresponding to wave vectors $\mathbf{k}_1^R, \mathbf{k}_2^R, \mathbf{k}_3^R, \mathbf{k}_4^R$, respectively). The matrices, describing the way in which this set of four basis functions is transformed into different linear combinations of themselves under application of an arbitrary element of the space group G , are the matrices of the irr. rep. of group G associated with the wave vector \mathbf{k}^R . The dimension of this representation is equal to the number of wave vectors in the star—that is, to the number of basis functions, which are themselves the components of the order parameter corresponding to the transition.

We have checked that the I, II, and IV Landau conditions for the second-order phase transition are fulfilled in this case. If the irr. rep. found for G satisfies the III Landau condition (concerning nonexistence

of the third-order invariants in expansion of Gibbs free energy as power series in order-parameter components) the equilibrium structures can be obtained by extremization and minimization of the symmetry invariant expansion.

A cubic invariant that remains unchanged under all symmetry operations of space group G is generally constructed of products made of any three basis functions. For such a product to be invariant under the translations of G , the sum of the three corresponding wave vectors from the four-ray star should be equal to a reciprocal lattice vector of the high symmetry structure (should transform as the identical representation). We are easily convinced that in this case ($\{\mathbf{k}^R9\}$ star) third-order invariants cannot exist and thus all the Landau conditions for a continuous phase transition are met.

Having experimentally determined the high- and low-symmetry structures of the cage sublattice of stoichiometric cuprous selenide and comparing them with Tables 3.1 and 3.2 from (13), we have avoided the tedious extremization and minimization of the symmetry invariant expansion of Gibbs free energy. The observed structure obviously corresponds to a solution in which one of the order parameter components, $\eta_i = 1$ ($i = 1, 2, 3, 4$) and the other three are equal to zero (only one ray of the star $\{\mathbf{k}^R9\}$ is involved).

The value of the free energy in this minimum is independent of the actual choice of the nonzero η_i component. Provided that the thermodynamic variables upon which the expansion coefficients depend (pressure, temperature, etc.) are isotropic, all orientation variants can arise from the same phase transition with equal probabilities.

The number of translation variants \mathbf{T} (14) for a given rotation variant is given by the number of lattice nodes of the disordered α -phase structure within a primitive unit cell of the ordered β -phase structure, and can be obtained as the quotient of primitive unit cell volumes of the ordered (V_O) and disordered (V) phase, i.e., $\mathbf{T} = V_O/V$. In our case, $V_R = 2V_c$, so that within each of the four possible orientation variants, two translation variants are expected to occur.

Let us now consider the ordered β - Cu_2Se phase in its entirety—the ordered mobile cation subsystem within the deformed cage sublattice. The structure of stoichiometric cuprous selenide below 413 K is described as monoclinic (3) in terms of the double layer monoclinic supercell denoted by m , as well as the two four-layer “block cells” (M' , M'').

The transformation matrices are ($(\mathbf{a}_i, \mathbf{b}_i, \mathbf{c}_i) = (\mathbf{a}_{ci}, \mathbf{a}_{c2}, \mathbf{a}_{c3}) \cdot S_{ci}; i = m, M', M''$).

$$S_{cm} = \begin{bmatrix} \frac{1}{2} & -\frac{1}{2} & \frac{1}{2} \\ \frac{1}{2} & \frac{1}{2} & \frac{1}{2} \\ -1 & 0 & 1 \end{bmatrix},$$

$$\det S_{cm} = 3, V_m = 3a_c^3 = 12V_c$$

$$S_{cM'} = \begin{bmatrix} \frac{1}{2} & -\frac{1}{2} & 1 \\ \frac{1}{2} & \frac{1}{2} & 1 \\ -1 & 0 & 2 \end{bmatrix},$$

$$\det S_{cM'} = 6, V_{M'} = 6a_c^3 = 24V_c$$

$$S_{cM''} = \begin{bmatrix} \frac{1}{2} & -\frac{1}{2} & 1 \\ \frac{1}{2} & \frac{1}{2} & 1 \\ -1 & 0 & 1 \end{bmatrix},$$

$$\det S_{cM''} = 6, V_{M''} = 6a_c^3 = 24V_c.$$

We apply the same procedure as before to calculate the \mathbf{j} matrices ($\mathbf{j}_i = S_{ci}^{-1} \mathbf{g} S_{ci}$;

$i = m, M', M''; \mathbf{g} \in G_O$) and check for the conserved symmetry elements within the β -phase structure. The obtained \mathbf{j} matrices disclose that only two symmetry elements remain—the identity E and the σ_y mirror plane, except within the m reference frame where two extra symmetry elements arise, recognized as $U_{\bar{x}z} = \sigma_{\bar{x}z}I$ and σ_{xz} , contradicting the reported space group C_s^3 (Cm). Careful reexamination of the original (3, 5) Weissenberg photographs reveals that the relationship between the monoclinic supercell and the cubic subcell can be described by the matrix

$$S_{cm'} = \begin{bmatrix} \frac{1}{2} & -\frac{3}{2} & 1 \\ \frac{1}{2} & \frac{3}{2} & 1 \\ -1 & 0 & 0 \end{bmatrix}, \det S_{cm'} = 3.$$

Within this chosen m' reference frame, only E and σ_y are conserved, confirming the $C_s(m)$ point group symmetry.

The basis vectors of all these monoclinic lattices can be easily expressed as linear combinations of cubic primitive vectors with integral coefficients and thus the translations are a subgroup of translations of the cubic disordered structure.

As already shown, the point group of the ordered phase, denoted as J_O , is $C_s(m)$, which is a subgroup of G . Thus, the space group of the low-temperature stoichiometric copper selenide meets the group-subgroup I condition of Landau.

The basis functions of the representation with $\mathbf{k}^R = (2\pi/a_c) (\frac{1}{2}\frac{1}{2}\frac{1}{2})$ are also invariant for monoclinic translations, but if they were used for describing the low-temperature structure, its symmetry would be higher than actually observed.

Besides a doubling of the periodicity in the $[111]_c$ direction, the oscillation photographs taken in $\beta\text{-Cu}_2\text{Se}$ phase reveal [weak spot layer lines (3)] a tripling of the periodicity along the cubic $[\bar{1}10]_c$ direction [$\mathbf{b}_{\text{mon.}} = 3(\mathbf{a}_1 - \mathbf{a}_2)$]. This corresponds to the wave vector $\mathbf{k}^m = (2\pi/a_c) (\frac{1}{3}\frac{1}{3}0) = \mu(\mathbf{a}_1^* - \mathbf{a}_2^*) = \mathbf{b}_{\text{mon.}}^*$, with $\mu = \frac{1}{6}$. This \mathbf{k} point is not a

special symmetry point in the Brillouin zone and could lie anywhere along the line between the Γ and K points, retaining the same symmetry (the value of μ need not by reasons of symmetry be precisely $\frac{1}{6}$). It does not satisfy the IV condition of Landau ($-\mathbf{k}^m = \mathbf{k}^m + (2\pi/a_c)(\frac{2}{3}\bar{0}0)$). A second-order transition is still possible, but with the resulting state of lower symmetry that could not be described by a three-dimensional space group (8), that is, with loss of the three-dimensional periodicity of the lattice.

The function $\exp(i\mathbf{k}^m\mathbf{r}) = \exp(i\frac{2}{3}\pi(-x + y))$ is a basis function for the translational symmetry operations. The basic translations of monoclinic lattices leave it unchanged, while the lost translations of cubic structure multiply it by the factor $\exp(\pm i(\pi/3))$.

The group of the wave vector is $C_3(m)$. The star contains 12 vectors: $\mathbf{k}_1^m = (2\pi/a_c)(\frac{1}{3}\bar{1}0)$, $\mathbf{k}_2^m = (2\pi/a_c)(\frac{1}{3}0\bar{1})$, $\mathbf{k}_3^m = (2\pi/a_c)(\frac{1}{3}0\bar{1})$, $\mathbf{k}_4^m = (2\pi/a_c)(\frac{1}{3}0\bar{1})$, $\mathbf{k}_5^m = (2\pi/a_c)(0\frac{1}{3}\bar{1})$, $\mathbf{k}_6^m = (2\pi/a_c)(0\frac{1}{3}\bar{1})$, $\mathbf{k}_7^m = -\mathbf{k}_1^m$, $\mathbf{k}_8^m = -\mathbf{k}_2^m$, $\mathbf{k}_9^m = -\mathbf{k}_3^m$, $\mathbf{k}_{10}^m = -\mathbf{k}_4^m$, $\mathbf{k}_{11}^m = -\mathbf{k}_5^m$, $\mathbf{k}_{12}^m = -\mathbf{k}_6^m$, (since \mathbf{k}_7^m and $-\mathbf{k}_7^m$ differ by a vector that is not a cubic reciprocal lattice vector).

All the wave vectors in the star can be obtained from \mathbf{k}_1^m as a result of action of rotational symmetry operators of G not conserved in J ($E\mathbf{k}_1^m = \mathbf{k}_1^m$, $C_{2y}\mathbf{k}_1^m = \mathbf{k}_2^m$, $C_{3,1}^{-1}\mathbf{k}_1^m = \mathbf{k}_3^m$, $C_{3,2}^{-1}\mathbf{k}_1^m = \mathbf{k}_4^m$, $C_{3,4}^{-1}\mathbf{k}_1^m = \mathbf{k}_5^m$, $C_{3,3}^{-1}\mathbf{k}_1^m = \mathbf{k}_6^m$, $C_{2x}\mathbf{k}_1^m = \mathbf{k}_8^m$, $C_{3,3}^1\mathbf{k}_1^m = \mathbf{k}_9^m$, $C_{3,4}^1\mathbf{k}_1^m = \mathbf{k}_{10}^m$, $C_{3,1}^1\mathbf{k}_1^m = \mathbf{k}_{11}^m$, $C_{3,2}^1\mathbf{k}_1^m = \mathbf{k}_{12}^m$) which form the point group $T(23)$ (variant generating group).

We can represent $G_0 \equiv T_d$ as the semidirect product $T_d = T \wedge C_3$, the decomposition into left cosets of J_0 ($= \{[E], [\sigma_{xy}]\}$) being

$$G_0 = EJ_0 + C_{2x}J_0 + C_{2y}J_0 + C_{2z}J_0 + C_{3,1}^1J_0 + C_{3,2}^1J_0 + C_{3,3}^1J_0 + C_{3,4}^1J_0 + C_{3,1}^{-1}J_0 + C_{3,2}^{-1}J_0 + C_{3,3}^{-1}J_0 + C_{3,4}^{-1}J_0 = T \wedge C_3.$$

Applying the coset representatives $\mathbf{g}_i \in T$ to the structure of the low-symmetry mono-

clinic phase gives 12 structures of symmetry $\mathbf{g}_iJ_0\mathbf{g}_i^{-1}$ (Table II). The monoclinic point group J_0 can adopt six different orientations within the point group T_d (listed exactly with respect to the symmetry elements of T_d):

$$\begin{aligned} J_1 &= \{[E], [\sigma_{xy}]\} \\ J_2 &= \{[E], [\sigma_{\bar{x}y}]\} \\ J_3 &= \{[E], [\sigma_{xz}]\} \\ J_4 &= \{[E], [\sigma_{\bar{x}z}]\} \\ J_5 &= \{[E], [\sigma_{yz}]\} \\ J_6 &= \{[E], [\sigma_{\bar{y}z}]\}, \end{aligned}$$

but each J_i ($i = 1-6$) occurs twice, associated with wave vectors \mathbf{k}_i^m (J_i) and $-\mathbf{k}_i^m = \mathbf{k}_{i+6}^m$ ($J_i^* = J_{i+6}$). Reexamination of Fig. 2 shows that the point groups of each of the four rhombohedral orientation variants H_i ($i = 1-4$) can be formed by taking together the symmetry operations of the appropriate three monoclinic orientation variants which differ by $\pm 120^\circ$ rotations around a threefold axis of the cubic cage. Indeed, if we construct the possible sums of three vectors from the 12-ray star of \mathbf{k}^m (guided by the correspondence of \mathbf{k}_i^m 's and J_i 's in Fig. 2 and including different signs), we arrive at eight combinations summing up to wave vectors proportional to the rays of the star of \mathbf{k}^R :

$$\begin{aligned} \pm(\mathbf{k}_2^m + \mathbf{k}_4^m + \mathbf{k}_6^m) &\propto \pm\mathbf{k}_1^R \Rightarrow H_1 \\ \pm(\mathbf{k}_2^m + \mathbf{k}_3^m + \mathbf{k}_5^m) &\propto \mp\mathbf{k}_4^R \Rightarrow H_2 \\ \pm(\mathbf{k}_1^m - \mathbf{k}_3^m + \mathbf{k}_6^m) &\propto \mp\mathbf{k}_2^R \Rightarrow H_3 \\ \pm(\mathbf{k}_1^m - \mathbf{k}_4^m + \mathbf{k}_5^m) &\propto \pm\mathbf{k}_3^R \Rightarrow H_4. \end{aligned}$$

The point group of the resulting wave vectors is C_{3v} . This means that three simultaneously observed (3) monoclinic orientation variants mutually related by rotations around the third-order cubic axis contribute to the diffraction pattern displaying the pseudorhombohedral symmetry of the structure domain coupled to one of four possible cage distortion directions.

TABLE II
FOR $\mathbf{g} \in G_0$, $J_j = \mathbf{g}^{-1} J_j \mathbf{g}$ (E.G., FOR $i = 1; j = 1-6$)

\mathbf{g}^{-1}	\mathbf{g}	\mathbf{g}^{-1}	\mathbf{g}	\mathbf{g}^{-1}	\mathbf{g}	\mathbf{g}^{-1}	\mathbf{g}	\mathbf{g}^{-1}	\mathbf{g}	\mathbf{g}^{-1}	\mathbf{g}
E	E	C_{2x}	C_{2x}	$C_{3,1}^{-1}$	$C_{3,1}^1$	$C_{3,2}^{-1}$	$C_{3,2}^1$	$C_{3,4}^{-1}$	$C_{3,4}^1$	$C_{3,2}^{-1}$	$C_{3,2}^1$
C_{2z}	C_{2z}	C_{2y}	C_{2y}	$C_{3,3}^{-1}$	$C_{3,3}^1$	$C_{3,4}^{-1}$	$C_{3,4}^1$	$C_{3,1}^{-1}$	$C_{3,1}^1$	$C_{3,3}^{-1}$	$C_{3,3}^1$
σ_{yz}	σ_{xy}	S_{4z}^{-1}	S_{4z}^1	σ_{yz}	σ_{yz}	σ_{yz}	σ_{yz}	σ_{xz}	σ_{xz}	σ_{xz}	σ_{xz}
σ_{xz}	σ_{xy}	S_{4z}^1	S_{4z}^{-1}	S_{4x}^{-1}	S_{4x}^1	S_{4x}^{-1}	S_{4x}^1	S_{4y}^{-1}	S_{4y}^1	S_{4y}^{-1}	S_{4y}^1
$\mathbf{g}^{-1} J_1 \mathbf{g} = J_1$		$\mathbf{g}^{-1} J_1 \mathbf{g} = J_2$		$\mathbf{g}^{-1} J_1 \mathbf{g} = J_3$		$\mathbf{g}^{-1} J_1 \mathbf{g} = J_4$		$\mathbf{g}^{-1} J_1 \mathbf{g} = J_5$		$\mathbf{g}^{-1} J_1 \mathbf{g} = J_6$	
$\mathbf{g}^{-1} \in EJ_1$		$\mathbf{g}^{-1} \in C_{2x} J_1$		$\mathbf{g}^{-1} \in C_{3,1}^{-1} J_1$		$\mathbf{g}^{-1} \in C_{3,2}^{-1} J_1$		$\mathbf{g}^{-1} \in C_{3,4}^{-1} J_1$		$\mathbf{g}^{-1} \in C_{3,2}^{-1} J_1$	
$\in C_{2z} J_1$		$\in C_{2y} J_1$		$\in C_{3,3}^{-1} J_1$		$\in C_{3,4}^{-1} J_1$		$\in C_{3,1}^{-1} J_1$		$\in C_{3,3}^{-1} J_1$	

The point group of the wave vector \mathbf{k}^m is equal to the point group of the monoclinic structure, so that the basis functions are symmetric under the rotational symmetry operations and transform as the totally symmetric small rep. associated with the star of \mathbf{k}^m . The irr. rep. of the entire space group G is 12-dimensional and is essentially real since the set of base functions consists of $\exp(\frac{2}{3}i\pi(-x+y))$, $\exp(\frac{2}{3}i\pi(x+y))$, $\exp(\frac{2}{3}i\pi(x-z))$, $\exp(\frac{2}{3}i\pi(x+z))$, $\exp(\frac{2}{3}i\pi(y-z))$, $\exp(\frac{2}{3}i\pi(y+z))$, and their complex conjugates.

We still have to consider the possible existence of cubic invariants in the expansion of free energy. Each of the 12 wave vectors in the star is related to two others by rotations for $\pm 120^\circ$ around the cubic third-order axis (monoclinic \mathbf{c}^* direction). Such three-coplanar wave vectors perpendicular to $\mathbf{c}_{\text{mon.}}^*$ sum up exactly to zero in eight combinations (denoted by ray numbers, using the convention $i^* = i + 6$):

$$\begin{aligned} 1 + 3 + 5^* &= 1^* + 3^* + 5 = 1 + 4 + 6^* \\ &= 1^* + 4^* + 6 = 2^* + 3 + 6 = 2 + 3^* \\ &+ 6^* = 2^* + 4 + 5 = 2 + 4^* + 5^* = 0. \end{aligned}$$

The corresponding products of basis functions form a third-order invariant, the existence of which does not allow the phase transition to be of the second order.

In order to determine the number of translation variants within a given monoclinic orientation variant, we make use of the transformation matrices relating the base vectors of the ordered and disordered structure, thus obtaining $\mathbf{T}_m = 6$, $\mathbf{T}_M = 12$.

Experimental

Microfurnace for the Weissenberg Goniometer

Such a variety of intrinsically possible structural complexities led us to developing a heating device for a Weissenberg camera that would permit single-crystal X-ray analysis to be carried out as a function of temperature. Having at our disposal a commercial Weissenberg camera ("Siemens," film diameter ϕ 57.3 mm) suitable for recording single-crystal diffraction data on rotation, oscillation, and equi-inclination Weissenberg photographs, we were naturally led to select a heating device designed to allow the full usage of these instrument facilities, extending its applicability to cover the entire temperature range of interest. Bearing in mind some of the requirements to be fulfilled, namely, to ensure accurate and constant crystal settings about the rotation axis, to avoid as much as possible screening of the direct and diffracted beams, and to provide for precise temperature measurement

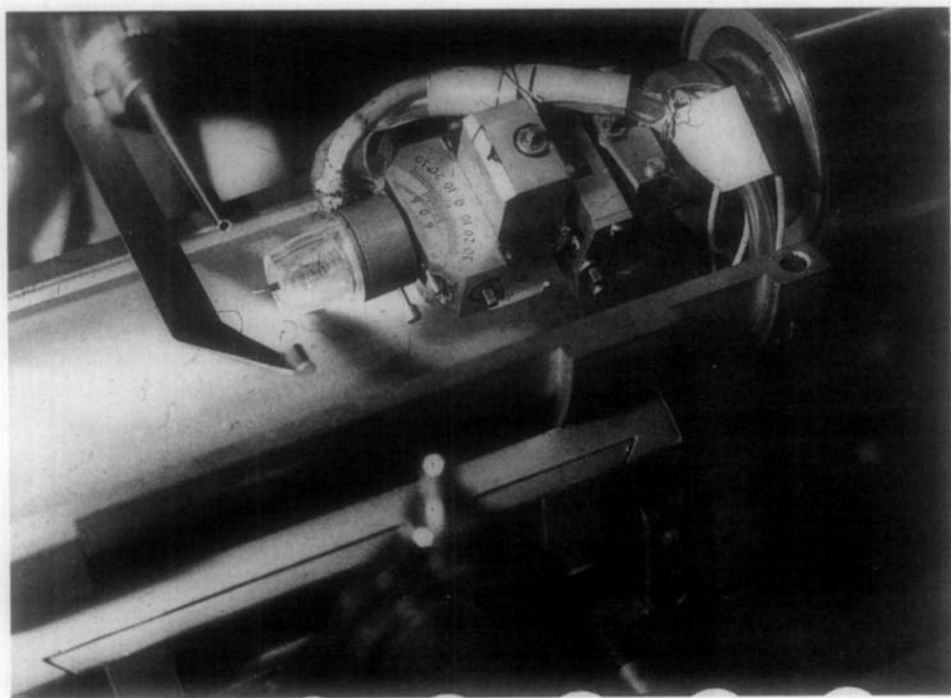


FIG. 3. Microfurnace mounted on Weissenberg goniometer.

and its long-term stability, we followed, with slight modifications, the microfurnace design given by Tuinstra and Fraase Storm (17).

The microfurnace with the sample mounted on it is attached to the custom-made sledge, replacing the original one on a standard goniometer head, thus enabling vertical, lateral, and rotational adjustments of the sample position (Fig. 3). The single-crystal or powder specimen is sealed in an evacuated quartz capillary inserted axially into the metal tube in the furnace center containing the temperature sensor [an oxidation-resistant platinum (18) alloy thermocouple]. The sample is heated by a hot air jet enclosed coaxially with a cylindrical cool air stream, the air flow being supplied by a pair of aquarium pumps (19) at a constant rate of 4 liters min^{-1} . The voltage from the thermocouple measuring the hot jet temperature is fed to an electronic temperature

regulator (20), where it is amplified and compared with a preset reference voltage. The power output to the Kanthal wire heater is varied proportionally to the detected temperature deviation from the selected value, giving a thermal stability of better than ± 0.25 K.

Using another thermocouple, we investigated the axial temperature distribution, showing the temperature gradient ranging from 0.5 to 5 K mm^{-1} along the axis. The samples are intentionally not placed in the smallest gradient region, as it would produce obscuring of almost half of an oscillation photograph by the muzzle of the furnace. A compromise of having a temperature gradient of at most 4 K mm^{-1} at 600 K (probably smaller across a typical 0.5-mm-long single crystal, due to thermal equalization) and only one-third of an oscillation photograph screened out has been considered acceptable.

The absolute value of temperature was checked *in situ* by measuring the lattice constant from silver powder diffraction patterns at different temperatures. The sample temperature deviates reproducibly for up to 5% of the value measured with the sensor thermocouple in the operation range from room temperature to 900 K.

As the hot air is let out axially through a hole made in the layer-line screen holder, no film heating was observed even after the 48-hr exposures at elevated temperatures. The film holder was made of two semicylindrical halves, permitting the film exchange as well as any necessary readjustments of the crystal setting without disturbing the sample temperature.

Sample Preparation

The compound preparation was described earlier by Vučić and Ogorelec (21). Suitable single-crystal specimens, fitting the quartz capillary sample holder, were cleaved off from polycrystalline ingots obtained by the Bridgeman method. The crystal habit of the samples closely resembles that shown in Fig. 1. of Ref. (3).

Results and Discussion

We followed the structural changes of stoichiometric Cu_2Se macroscopic single crystals, taking the zero- and higher-layer Weissenberg photographs in the temperature interval from 430 to 300 K, that is, above and below the ordering $\alpha \rightarrow \beta$ transition temperature (413 K).

The high-temperature α -phase photographs displayed the well-known cubic pattern (Fig. 4a). After the samples were cooled through the ordering $\alpha \rightarrow \beta$ transition, the superstructural spots, indicating the doubling of periodicity along the $[111]_c$ direction, appeared. Some samples showed this feature dominantly along only one of the $\langle 111 \rangle_c$ axes, while for the others it was equally well pronounced along both $\langle 111 \rangle_c$

axes, which can be seen within a single Weissenberg photograph of a crystal rotating around the $[\bar{1}10]_c$ axis (Fig. 4b).

As already mentioned, the choice of any of body cube diagonals as the direction of the rhombohedral deformation upon the $\alpha \rightarrow \beta$ transition would be equally probable if there were no external influences. But, during the phase transition, the real crystals are subject to different anisotropic fields and temperature gradients due to imperfections in crucible shape and nonuniform heating. These could result in singling out some preferred orientations for the cage distortion to occur upon the $\alpha \rightarrow \beta$ transition.

In the oscillation photographs taken just below the transition temperature, the weak spot higher layer lines (indicating the tripled periodicity along the $[\bar{1}10]_c$ oscillation axis) confirm the simultaneous onset of structure changes described by two nonequivalent wave vectors, \mathbf{k}^m and \mathbf{k}^m . As it is not possible to construct a single wave vector that would describe the transition to the observed β -phase structure [the $(\mathbf{k}^R \pm \mathbf{k}^m)$ wave vector would have lower proper symmetry ($\equiv \{E\}$) than observed], the transition does not correspond to a single irreducible representation. Thus, it violates the II condition of Landau, in accordance with the experimentally observed first-order character of the phase transition (3, 4).

A gain of further information about the monoclinic superlattice orientation variants was prohibited by the pronounced weakening of already weak spots of the higher layer lines due to the absorption of the quartz capillary enclosing the tiny single crystal.

Summary

Starting from the experimental findings about the rather intricate structure of the β phase of stoichiometric cuprous selenide, we considered separately two major components of the symmetry lowering at the $\alpha \rightarrow$

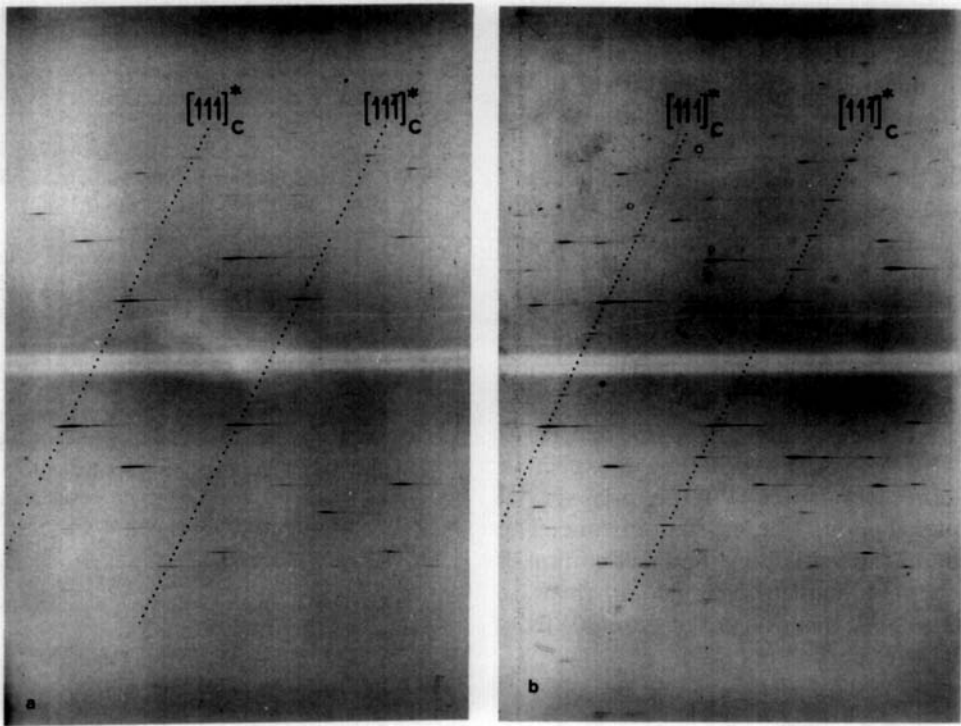


FIG. 4. Sections of Weissenberg photographs of a Cu_2Se single crystal displaying the $(\mathbf{a}^* + \mathbf{a}_1^*, \mathbf{a}_2^*)$ plane (cubic notation): (a) in the high-temperature α phase; (b) in the β phase with two orientation variants visible, developed along $[111]_c^*$ and $[11\bar{1}]_c^*$.

β phase transition: the rhombohedral deformation of the cage sublattice and the ordering of the mobile cation subsystem.

Having identified the wave vector that describes the cage sublattice symmetry reduction, we confirmed by applying the Landau theory of phase transitions that the rhombohedral elongation of the cage along a body cube diagonal observed in the β phase is indeed the equilibrium structure. It is expected to appear in four equivalent and equally probable orientation variants corresponding to four rays in the star of the wave vector. The simultaneous presence of these variants upon the $\alpha \rightarrow \beta$ transition was detected using a microfurnace attachment for the Weissenberg goniometer.

Application of group-theoretical methods

to the other change of periodicity characteristics for the $\alpha \rightarrow \beta$ first-order phase transition leads to the possibility of 12 monoclinic orientation twins corresponding to 12 rays in the star of the appropriate wave vector. Their simultaneous appearance in groups of three coupled to the cage rhombohedral distortion direction seems quite natural, considering the pseudorhombic symmetry such a set displays. The existence of these variants was deduced from ED patterns in (3). The diffuseness of the nearly continuous weak spot rows, easily noted in those patterns, suggests the presence of a stacking disorder of monoclinic variants along the pronounced $[111]_c$ direction. This, as well as the limited spatial extending of a single domain, is clearly visible in the high-

resolution lattice image of Cu_2Se in (22). The investigation of their probable long-range ordering as a function of temperature and time suggests more subtle experimental techniques.

The types of ordering discussed here are not uncommon in FCC materials, particularly those that can exhibit nonstoichiometry. Our attention has been drawn to the striking correspondence between the wave vectors relevant for symmetry lowering in copper selenide and those found in the early transition-metal sulfides with the NaCl-type structure [for example, Zr_{1-x}S , see (23)]. The \mathbf{k}^{R} wave vector is not to be unexpected, as it corresponds to one of the three special symmetry points of the Brillouin zone. The \mathbf{k}_m vector (not satisfying the IV condition of Landau) could give rise to incommensurate structure, but this was not discernable from available experimental data.

Acknowledgments

This work was supported by the Selfmanaging Community of Interest for Scientific Research of SR Croatia.

References

1. P. RAHLFS, *Z. Phys. Chem. B* **31 H3**, 157 (1936).
2. W. BORCHERT, *Z. Kristallogr. Kristallgeom. Kristallphys. Krystalchem.* **106**, 5 (1945).
3. O. MILAT, Z. VUČIĆ, AND B. RUŠIĆ, *Solid State Ionics* **23**, 431 (1987).
4. Z. VUČIĆ, O. MILAT, V. HORVATIĆ, AND Z. OGOR-ELEC, *Phys. Rev. B* **24**, 5398 (1981).
5. J. GLADIĆ, "Graduation Thesis," Zagreb (1983).
6. L. D. LANDAU AND E. M. LIFSHITZ, "Statistical Physics," Pergamon, Oxford (1980).
7. H. F. FRANZEN, "Second-Order Phase Transitions and the Irreducible Representation of Space Groups," Springer-Verlag, Berlin (1982).
8. C. HAAS, *Phys. Rev. A* **140**, 863 (1965).
9. R. A. EVARESTOV AND V. P. SMIRNOV, *Metodi teorii grup v kvantovoi himii tverdogo tela*, Izdatel'stvo Leningradskogo Universiteta, Leningrad (1987).
10. E. F. BERTAUT, Y. LE FUR, AND S. ALÉONARD, *J. Solid State Chem.* **73**, 556 (1988).
11. G. F. KOSTER, J. O. DIMMOCK, R. G. WHEELER, AND H. STATZ, *Properties of the Thirty-Two Point Groups*, MIT Press, Cambridge, MA (1963).
12. O. V. KOVALEV, *Irreducible Representations of the Space Groups*, Gordon & Breach, New York (1965).
13. J. A. IZJUMOV AND V. N. SIROMJATNIKOV, *Fazovye perekhodi i simetrija kristalov*, Nauka, Moskva (1984).
14. G. VAN TENDELOO AND S. AMELINCKX, *Acta Crystallogr. Sect. A* **30**, 431 (1974).
15. H. T. STOKES AND D. M. HATCH, *Phys. Rev. B* **31**, 7462 (1985).
16. M. GUYMONT, *Phys. Rev. B* **18**, 5385 (1978).
17. F. TUINTRA AND G. M. FRAASE STORM, *J. Appl. Crystallogr.* **11**, 257 (1978).
18. G. S. BRADY, H. R. CLAUSER, *Materials Handbook*, 11th ed., McGraw-Hill, New York (1977).
19. F. A. UNDERWOOD AND B. F. CHAPMAN, *J. Appl. Crystallogr.* **9**, 258 (1976).
20. F. LISSALDE, S. C. ABRAHAMS, AND J. L. BERNSTEIN, *J. Appl. Crystallogr.* **11**, 31 (1978).
21. Z. VUČIĆ AND Z. OGOR-ELEC, *Philos. Mag. B* **42**, 287 (1980).
22. S. KASHIDA AND J. AKAI, *J. Phys. C* **21**, 5329 (1988).
23. H. F. FRANZEN AND J. C. W. FOLMER, *J. Solid State Chem.* **51**, 396 (1984).